Fracture detection through seismic cube orthogonal decomposition

Ivan Priezzhev* and Aaron Scollard, Schlumberger

Summary

We propose to use 3D orthogonal decomposition of the seismic cube flattened along the target layer to detect fractures and subtle faults or other latent features under strong noise conditions. The technology is based on principal component analysis (PCA) using computation of eigenvalues and eigenvectors of the 3D autocorrelation function of the original seismic cube. Each orthogonal component is also a cube, and their sum is very close to that of the original cube. Orthogonality means the correlation coefficient between any two components will be about zero. Since the noise and acquisition footprints have no correlation with fractures or faults, reflections or other latent features, they stand out as separate orthogonal components. Wellbore information is usually required to select an orthogonal component useful for fracture detection. Fault and fracture auto tracking technology such as Ant-Tracking (Pedersen *at al.,* 2002) can be applied to the selected orthogonal cube to improve the fracture image.

Introduction

This paper continues our investigation into orthogonal decomposition analyses of seismic data; in 2012 we proposed to use seismic surface (reflected horizon) orthogonal decomposition to detect fractures and other latent structures (Priezzhev and Scollard, 2012). Seismic cube latent structure analyses to detect faults, fractures, and latent reflections in noisy conditions are priority tasks for oil and gas exploration and production (E&P). The results of these analyses can be used for well placement, geologic modeling, sill analyses, detection of fractured zones or fracture corridors, and in E&P for unconventional resources and carbonate fields.

Fracture corridors or subtle faults are usually recognizable in seismic data as small-amplitude self-incoherent features on cross sections and as lineaments on slices or seismic surfaces. Many edge detection seismic attributes are used in industry to detect these features in a seismic cube or on a seismic reflection surface. The list of most used are the following: local angle and azimuth angle (Dalley et al., 1989; Marfurt, 2006); minimum, maximum, Gaussian curvature, and others (Flynn and Jain, 1989; Roberts, 2001; Chopra and Marfurt, 2007a); coherence; 3D curvatures; spectral decomposition (Chopra and Marfurt, 2007b, 2009). A common problem exists for conventional fracture- and fault-detection technologies: sensibility to the noise and acquisition footprint in seismic data. To eliminate noise and acquisition footprints in seismic data and to obtain information about faults and fractures, filters or smoothing is usually applied. This suppression of noise and acquisition footprints may at the same time remove small seismic features associated with faults and fractures.

Method

The theory of the proposed technology for analyzing the latent structure of a seismic cube through orthogonal decomposition is based on proper orthogonal decomposition (POD), also known as Karhunen–Loeve decomposition (KLD) or principal component analysis (PCA) (Pearson, 1901; Nikitin, 1986; Kirlin and Done, 1999; Liang *et al.*, 2002; Rathinam and Petzold, 2003; Luo *et al.*, 2007).

Commonly, PCA is used to analyze multidimensional measurements and to reduce the dimension and for latent factor analysis (Nikitin, 1986; Nikitin and Petrov, 2010; Koval *et al.*, 1984, 1987). PCA is also used for the analysis of images, including those of the seismic wave field (Kirlin and Done, 1999; Scheevel and Payrazyan, 1999). Nikitin and Petrov (Nikitin, 1986; Nikitin and Petrov, 2010) applied the first principal component in moving windows for optimal adaptive filtration.

The calculation of principal components reduces to the calculation of eigenvectors and eigenvalues of the 3D autocorrelation function of the original cube. According to the algorithm the orthogonal cubes will be sorted by their contribution to the total variance (amplitude) of the studied cube. The calculation of a 3D autocorrelation function means calculations of the correlation factors between the original seismic cube with the same cube but shifted in different directions (inline, crossline and trace) and lags. In other words, we use multiattribute analyses but all the attributes present the same shifted cube. In this case, to obtain all attributes, we read all values of the original seismic cube on moving 3D windows (subcube). Maximum lags have to be equal or bigger than the objects to be detected. At the core of PCA is this equation:

$$\Lambda = \Phi^T C \Phi \text{ ,} \qquad (1)$$

where C is the covariance matrix for the multidimensional vector X. In our case C is a 3D autocorrelation function of the cube according to predefined maximum lags. Φ is the matrix of eigenvectors that are orthogonal to each other, and Λ is the diagonal matrix of eigenvalues. The main property of the PCA is that the eigenvectors that correspond to principal components are uncorrelated, which is equivalent to orthogonality. The eigenvector corresponding to the maximum eigenvalue of the covariance matrix determines the first principal component, which is considered a background factor. The following is the computation equation:

$$o_{ijk}^r = \frac{\lambda^r (s_{\max} - s_{\min})}{NML\sqrt{\lambda^r}} \sum_{n=-N/2}^{N/2} \sum_{m=-M/2}^{M/2} \sum_{k=-L/2}^{L/2} \frac{(s_{i+n,j+m,k+l} - s_{avr})}{(s_{\max} - s_{\min})} \phi_{n,m,l}^r \text{ , } (2)$$

where o_{ijk}^r is r orthogonal component for i, j trace and k sample on the cube. $s_{i+n,j+m,k+l}$ is seismic sample values for i, j trace and k sample on the cube, where n, m, l are lags in i, j and k directions. N, M, L are maximum lags. s_{avr}, s_{max}, and s_{min} are average, maximum, and minimum cube amplitude values correspondingly. λ^r and $\phi_{n,m,l}^r$ are r eigenvalue and eigenvector correspondingly.

According to equation (1) and (2), we can calculate a set of orthogonal (noncorrelated) cubes with the sum very close to that of the original seismic cube. The next step needs to calibrate the results and to understand what each of the orthogonal cubes means and define one or several cubes that can be used like fracture- or fault- detection attributes. It can be done by a calibration procedure that is usually based on simple comparison of orthogonal cubes with other information about fractures, such as microimager measurements in wellbores or microseismic interpretation results. As practice shows, the first principal component accounts for up to 70 to 95% of the variance of the studied cube and reflects the main trend of the studied seismic cube amplitudes. Since the noise has no correlation with faults or other latent features in the cube, it stands out as separate principal components. By the same reasoning, the individual principal components will be footprints. Computations are organized so that the following decomposition of the original cube into orthogonal components and their sum is equal to that of the original cube.

According to the theory of PCA, this analysis is very similar to Fourier analyses (Kirlin and Done, 1999; Liang *et al.*, 2002; Rathinam and Petzold, 2003; Luo *et al.,* 2007) and the results also have very similar behavior. If a source cube or surface has features like "spikes" or "steps," it creates a very long set of orthogonal components with equal amplitude that is very similar to that of the "white spectrum." In this case, source data cannot be described as a "sparse signal" with limited spectrum, and such components are difficult to interpret. If the orthogonal decomposition analysis is fulfilled along seismic slices, it can intersect several different layers that can create a very big edge effect that is similar to the spikes or step features. It also can create a long set of orthogonal components with similar amplitude, which is difficult to interpret. So we recommend performing the analyses only along stratigraphic slices. In this case seismic amplitude will not be very different and the results can be included in just a small number of orthogonal components, which is much easier to interpret. To perform analyses on a thin layer with less than one seismic cycle, we recommend using 2D orthogonal decomposition technology for the top or bottom of the layer (Priezzhev and Scollard, 2012) or both 3D and 2D to get more stable results.

Synthetic example

Figure 1 shows an image of a 2D orthogonal decomposition example under strong noise and high-amplitude vertical and horizontal footprints. The fourth orthogonal component (figure 1.6) restores the image and the fifth and sixth components (figures 1.7, 1.8) can be used for edge detections of the image.
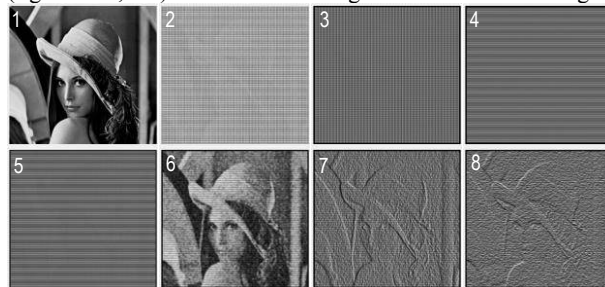

Figure 1: Image orthogonal decomposition example: 1) Source image. 2) Image (amplitude 256 units) with strong noise (amplitude 256 units) and high-amplitude vertical and horizontal footprint (amplitude 1000 units). 3), 4), 5), 6), 7), 8) First through sixth orthogonal components correspondingly.

To check the ability of the proposed technology and to detect small-amplitude seismic signals generated by fracturing under strong noise and footprint we use a 3D synthetic model. It is a sum of predefined cubes with trend, noise, footprint, and signal (Figure 2).
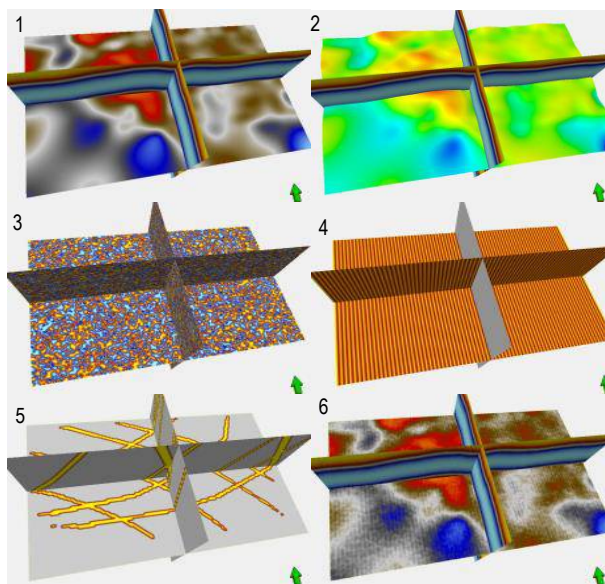

Figure 2: Synthetic model. 1) Trend cube, 2) Surface used to create trend cube. 3) Noise cube. 4) Footprint cube. 5) Fracture cube. 6) Sum of the trend cube (50 units), noise cube (3 units), footprint cube (3 units), and fracture signal cube (1.5 units).

Figure 2.1 shows a seismic cube that was used as a trend. The trend was made via the surface (figure 2.2) that was convoluted with low-frequency sinusoid. To create a synthetic cube (figure 2.6) we used a sum trend cube (figure 2.1) with amplitude of 50 units, noise cube (figure 2.3) with amplitude of 3 units, footprint cube (figure 2.4) with amplitude of 3 units, and "fracture corridors" cube with amplitude of 1.5 units (nonvertical model shown on figure 2.5).
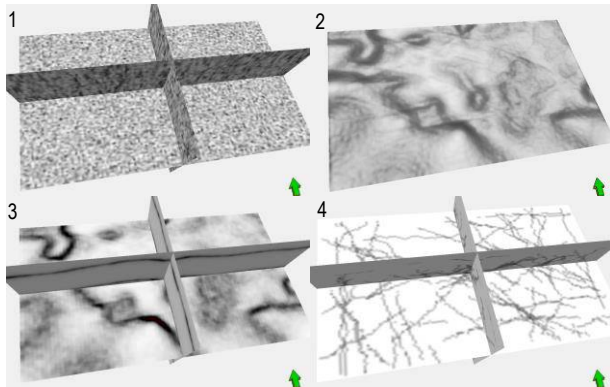
Figure 3: Conventional attributes calculated from synthetic model (figure 2.6). 1) 3D curvatures. 2) "Amplitude contrast" attribute (slice). 3) Variance cube. 4) Ant-Tracking (calculated via variance cube).

Figure 3 shows conventional attributes calculated from the synthetic model (figure 2.6). It is clearly seen that the attributes do not work to detect a useful signal in this very noisy condition. Only the "amplitude contrast" attribute (Boe, 2012) shows a very small footprint of the target signal on a few separate slices.
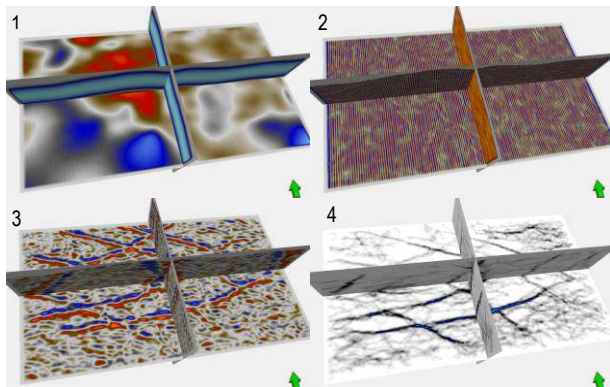

Figure 4: Results of orthogonal decomposition of the synthetic model (figure 2.6). 1), 2), 3) First through third orthogonal components correspondently. 4) Ant-Tracking attribute calculated using the third orthogonal component.

Figure 4 shows the orthogonal decomposition results obtained through seismic cube 3D analyses along the layer defined by the trend surface. The first orthogonal component restores a trend and the second restores the footprint. The third orthogonal component shows a very clear signal from modeled fractures. Other components show the noise. The Ant-Tracking attribute calculated using the third component also shows the signal and is compared with the conventional Ant-Tracking workflow, which is usually based on a variance cube and corresponds better to the signal (Figure 2.5).

Examples

Figures 5 and 6 show the proposed technology on a dataset from the Avalon shale, an unconventional shale play in

Delaware basin in New Mexico. Conventional Ant-Tracking attribute looks "geological" but does not correspond to the fracture direction calculated from the image results. The Ant-Tracking results calculated on the fourth orthogonal component look very continuous and fully correspond to the fracture directions observed from images in a well in the cube. The cross section with Ant-Tracking image in figure 6 shows non-vertical fracture direction, which corresponds with the seismic data.
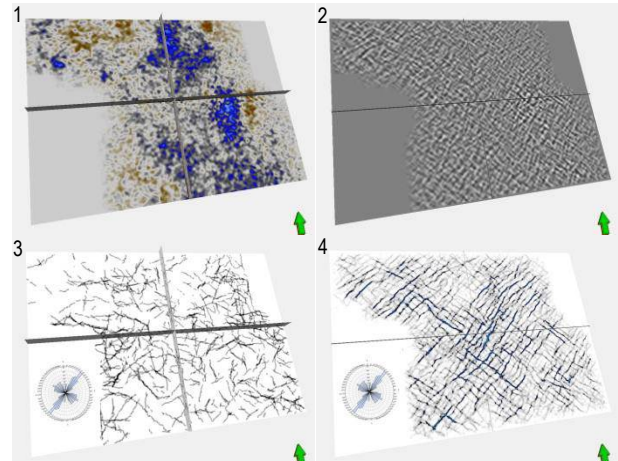

Figure 5: Avalon dataset example (courtesy of WesternGeco). 1) seismic cube. 2) Fourth orthogonal component. 3) Conventional Ant-Tracking and diagram of fracture direction from images. 4) Ant tracking calculated using the fourth component and fracture direction diagram.
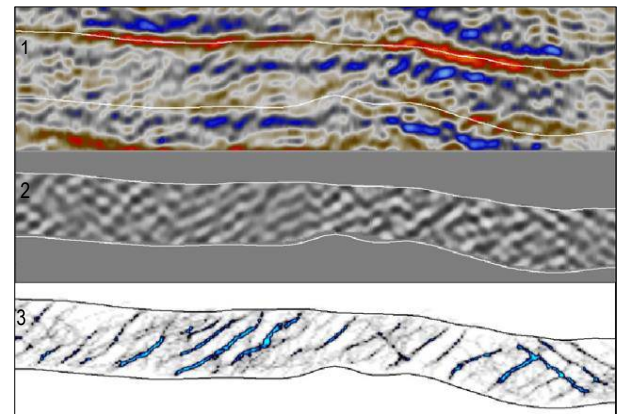

Figure 6: Avalon dataset example (courtesy of WesternGeco). 1) Seismic cross section from the center west-east section. 2) Fourth orthogonal component. 3) Ant-Tracking.

Figure 7 shows a dataset from the Barnett. Conventional Ant-Tracking calculated on a variance cube can be used to detect major faults in the region; however it will miss much of the detail around the smaller faults and fractures. Ant-Tracking calculated on the third orthogonal component identifies more faults and fractures that correspond to microseismic events. .
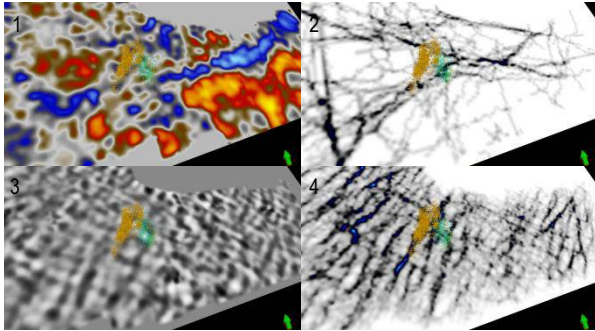
Figure 7: Barnett dataset example (courtesy of WesternGeco). 1) seismic slice. 2) Conventional Ant-Tracking results calculated on a variance cube. 3) Third orthogonal component. 4) Ant-Tracking calculated on third orthogonal component. All pictures include microseismic events; the colors show different stages.
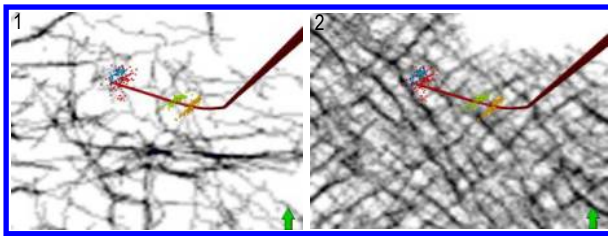

Figure 8: Montney dataset example (courtesy of WesternGeco). 1) Conventional Ant-Tracking results calculated on a variance cube. 2) Ant-Tracking calculated on 4th orthogonal component. All pictures include microseismic events; the colors show different stages.

Figure 8 shows the comparison of the conventional Ant-Tracking and Ant-Tracking calculated via orthogonal component. There is not any correlation with the microseismic events for the conventional Ant-Tracking and very good correlation for Ant-Tracking calculated on 4th orthogonal component.

Figure 9 shows a carbonate example. Both the fourth orthogonal cube and third orthogonal component calculated via seismic reflection surface at top of carbonate correlate with the image log results and can be used like seismic attributes to detect fracture corridors.
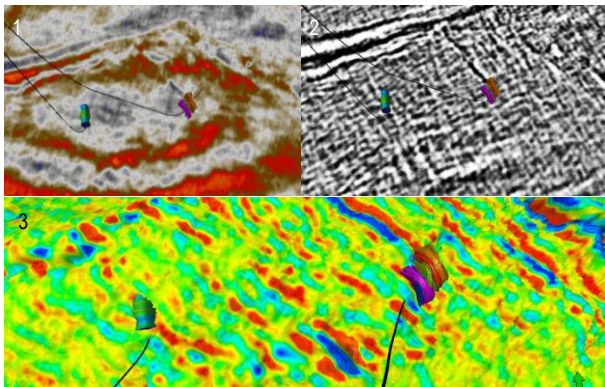

Figure 9: Seismic data from the Korchagin oil field in the Caspian Sea (courtesy of Lukoil NizhenevolzhskNeft). 1) Seismic slice near the top of carbonates. 2) Fourth orthogonal cube. 3) Third orthogonal

component calculated from reflection surface at the top of carbonates (2D decomposition). All pictures include two horizontal wells with image log interpretation results (right well) and density log (left well).

Conclusions

A new technology that applies the latent structure analysis of a seismic cube under conditions of strong noise and footprint is proposed. The technology is based on the orthogonal decomposition of the stratigraphically flattened 3D seismic cube. The components will be sorted according to their contribution to the total amplitude of the studied cube.

The main advantage of the method is the ability to assign uncorrelated noise or footprints and useful signals to different noncorrelated components (different seismic cubes). It is a different approach than a smoothing operation because it does not filter high-frequency information from the cube but separates it according to the shape.

To understand what every component means (noise or useful signal) it is necessary to calibrate the results. For this purpose it is recommended to use information about fractures and faults from different sources such as well logs and microseismic data. Additionally the Ant-Tracking attribute can be applied to the orthogonal component to improve the fracture image and to use the results for future fracture modeling.

To get the best results we propose to use the analyses along stratigraphic layers (along seismic horizons). Otherwise, if analyses are applied along seismic slices, only edge effects will be shown when a slice goes from one geological layer to the other.

Any image (satellite, geological, geophysical, or any other) also can be orthogonally decomposed to discover latent structure and to obtain a separate noncorrelated set of images (Figure 1). Another possible advantage of the proposed method is an ability to separate results of different geological processes that create orthogonal (uncorrelated) features in a seismic cube.

We believe that if a target layer is thin relative to seismic resolution (one or less of seismic cycles), 2D seismic surface analyses for the top or bottom of the layer are much preferred. The proposed technology has been tested on synthetic and real datasets.

The technology can be applied to detection of fracture corridors for unconventional resource exploration and for carbonate exploration under strong noise conditions.

Acknowledgments

EDITED REFERENCES

Note: This reference list is a copy-edited version of the reference list submitted by the author. Reference lists for the 2013 SEG Technical Program Expanded Abstracts have been copy edited so that references provided with the online metadata for each paper will achieve a high degree of linking to cited sources that appear on the Web.

REFERENCES

Boe, T., 2012, Enhancement of large faults with a windowed 3D radon transform filter: 82nd Annual International Meeting, SEG, Expanded Abstracts, 1–5.

Chopra, S., and K. J. Marfurt, 2007a, Volumetric curvature attributes for fault/fracture characterization: First Break, **25**, no. 7, 35–46.

Chopra, S., and K. J. Marfurt, 2007b, Seismic attributes for prospect identification and reservoir characterization: SEG.

Chopra, S., and K. J. Marfurt, 2009, Detecting stratigraphic features via cross-plotting of seismic discontinuity attributes and their volume visualization: The Leading Edge, **28**, 1422–1426, http://dx.doi.org/10.1190/1.3272695.

Dalley, R. M., E.C.A. Gevers, G. M. Stampfli, D. J. Davies, C. N. Gastaldi, P. A. Ruijtenberg, and G.J.O. Vermeer, 1989, Dip and azimuth displays for 3D seismic interpretation: First Break, **7**, no. 3, 86–95.

Flynn, P. J., and K. J. Jain, 1989, On reliable curvature estimation: IEEE Conference on Computer Vision and Pattern Recognition, 110–116.

Kirlin, R. L., and W. J. Done, 1999, Covariance analysis for seismic signal processing: Geophysical Developments no.8, SEG.

Koval, L. A., I. I. Priezzhev, and A. V. Ovcharenko, 1984, Interpretation of complex data based on recognition and classification in an automated system for processing airborne system: Geology and Geophysics, **9**, no. 277, 127–133.

Koval, L. A., A. V. Ovcharenko, and I. I. Priezzhev, 1987, Interpretation technology of complex airborne materials in the system ASOM-AGS/ES and the results of their use in Eastern Tuva: Geology and Geophysics, **6**, 81–92.

Liang, Y. C., H. P. Lee, S. P. Lim, W. Z. Lin, K. H. Lee, and C. G. Wu, 2002, Proper orthogonal decomposition and its applications — Part I: Theory: Journal of Sound and Vibration, **252**, no. 3, 527–544, http://dx.doi.org/10.1006/jsvi.2001.4041.

Luo, Z., J. Zhu, R. Wang, and I. M. Navon, 2007, Proper orthogonal decomposition approach and error estimation of mixed finite element methods for the tropical Pacific Ocean reduced gravity model: Computer Methods in Applied Mechanics and Engineering, **196**, no. 41–44, 4184–4195, http://dx.doi.org/10.1016/j.cma.2007.04.003.

Marfurt, K. J., 2006, Robust estimates of 3D reflector dip and azimuth: Geophysics, **71**, no. 4, 29–40, http://dx.doi.org/10.1190/1.2213049.

Nikitin, A. A., 1986, The theoretical basis of geophysical data processing: Nedra, 256.

Nikitin, A. A., and A. V. Petrov, 2010, Theoretical bases for statistical methods separation of geophysical anomalies: Russian State Geological University, 180.

Pearson, K., 1901, On lines and planes of closest fit to a system of points in space: Philosophical Magazine, **2**, 609–629.

Pedersen, S. I., T. Randen, L. Sonneland, and O. Steen, 2002, Automatic fault extraction using artificial ants: 72nd Annual International Meeting, SEG, Expanded Abstracts, 512–515.

Priezzhev, I. I., and A. Scollard, 2012, Fault and fracture detection based on seismic surface orthogonal decomposition: 74th Annual International Conference and Exhibition, EAGE, Extended Abstracts, W041.

Rathinam, M., and L. Petzold, 2003, A new look at proper orthogonal decomposition: SIAM Journal on Numerical Analysis, **41**, no. 5, 1893–1925, http://dx.doi.org/10.1137/S0036142901389049.

Roberts, A., 2001, Curvature attributes and their application to 3D interpreted horizons: First Break, **19**, no. 2, 85–100, http://dx.doi.org/10.1046/j.0263-5046.2001.00142.x.

Scheevel, J. R., and K. Payrazyan, 1999, Principal component analysis applied to 3D seismic data for reservoir property estimation: SPE Annual Technical Conference and Exhibition, SPE 56734.